Journal of Clinical and Translational Hepatology **2021** vol. 9(6) | 809–817
DOI: 10.14218/JCTH.2021.00021

Original Article

MicroRNA-7-5p Inhibits Migration, Invasion and Metastasis of Intrahepatic Cholangiocarcinoma by Inhibiting MyD88

Yi Tang#, Zhenyong Tang#, Jianrong Yang, Tianqi Liu and Yuntian Tang*

Department of Hepatobiliary Surgery, People's Hospital of Guangxi Zhuang Autonomous Region, Nanning, Guangxi, China

Received: 7 January 2021 | **Revised:** 29 March 2021 | **Accepted:** 8 April 2021 | **Published:** 10 May 2021

Abstract

Background and Aims: Intrahepatic cholangiocarcinoma (ICC) is a malignant tumor derived from intrahepatic bile duct epithelial cells. Accumulating studies report that microRNAs are widely involved in tumor migration and metastasis by regulation of target genes. miR-7-5p has been confirmed to inhibit tumor metastasis and to be related to prognosis for several malignant tumors. Our study investigated the underlying functions of miR-7-5p in ICC. ***Methods:*** The expression of miR-7-5p in ICC tissues but also in ICC cell lines was analyzed by real-time PCR. By analyzing the relationship between the clinicopathological parameters of 60 ICC patients and the expression level of miR-7-5p, the effect of miR-7-5p on the prognosis was clarified. After transfected with miR-7-5p mimics or miR-7-5p inhibitor, cell counting kit-8 assay was applied to evaluate the cells proliferation, flow cytometry was applied to analyze the cells apoptosis, wound healing assay and transwell chamber assay were applied to analyze the cell invasion and migration. A luciferase reporter assay was identified the relationship of miR-7-5p and myeloid differentiation factor 88 (MyD88). Western blotting was used to analyze the proteins expression. And immunochemistry was performed to determine the expression of MYD88 in ICC tissues. ***Results:*** Our data showed the expression of miR-7-5p was down-regulated not only in ICC tissues but also in ICC cell lines compared with normal controls. Low expression of miR-7-5p was notably associated with poor prognosis in ICC patients. miR-7-5p negatively regulated cell proliferation, migration, invasion and apoptosis in ICC cells. We further verified that MyD88 was a novel target of miR-7-5p and was significantly overexpressed in ICC tissues. Overexpression of MyD88 counteracted the effects of miR-7-5p in ICC cells. ***Conclusions:*** The present findings suggest that miR-7-5p plays a pivotal role in ICC invasion by regulating MyD88. Ampliative insight into the key factors of ICC invasion may result in the development of new treatment options for ICC.

Keywords: Intrahepatic cholangiocarcinoma; miR-7-5p; MyD88.

Abbreviations: ANTs, adjacent non-tumor tissue samples; CCK-8, cell counting kit-8; EMT, epithelial-mesenchymal transition; HCC, hepatocellular carcinoma; ICC, intrahepatic cholangiocarcinoma; IL-1R, interleukin 1 receptor; miRNAs, microRNAs; MyD88, yeloid differentiation factor 88; T-ALL, T cell acute lymphoblastic leukemia; TLR, toll-like receptor; UTR, untranslated region.

#Both authors contributed equally.

***Correspondence to:** Yuntian Tang, Department of Hepatobiliary Surgery, People's Hospital of Guangxi Zhuang Autonomous Region, Nanning, Guangxi, China. ORCID: https://orcid.org/0000-0001-7658-870X. Tel/Fax: +86-771-218-6308, E-mail: tang5620@sina.com

Citation of this article: Tang Y, Tang Z, Yang J, Liu T, Tang Y. MicroRNA-7-5p inhibits migration, invasion and metastasis of intrahepatic cholangiocarcinoma by inhibiting MyD88. J Clin Transl Hepatol 2021;9(6):809–817. doi: 10.14218/JCTH.2021.00021.

Introduction

Intrahepatic cholangiocarcinoma (ICC) is a very aggressive malignant tumor of the biliary tract, which is often diagnosed in the advanced stage.[1–2] Surgery is the main curative option. First-line chemotherapy is the preferred strategy in cases with macroscopic residual disease after surgery or locally recurrent or unresectable cholangiocarcinoma at the time of diagnosis.[3] However, the treatment effect is very poor. The long-term survival time of patients with unresectable ICC is very short, and the 5-year survival rate after diagnosis is less than 5% to 10%.[2,4] Therefore, it has important clinical significance for finding new prognostic indicators and therapeutic targets by exploring the molecular mechanism of the progression of ICC.[5–7]

MicroRNAs (miRNAs) are highly conserved small noncoding RNAs, with lengths of approximately 17–25 nucleotides. Recently, miRNAs have been shown to be involved in multiple steps that regulate the occurrence and development of ICC.[8] MiR-7-5p has been confirmed as exerting antitumor effects in multiple types of carcinomas, including breast cancer, pancreatic ductal adenocarcinoma, glioma, etc.[9–11] However, the underlying mechanisms and significance of miR-7-5p in ICC remain unclear.

Myeloid differentiation factor 88 (MyD88) mainly mediates the inflammatory response to cell injury as an adaptor protein binding to the Toll-like receptor (TLR) and interleukin 1 receptor (IL-1R).[12–14] Previous studies have shown that the abnormal expression of MyD88 is closely related to tumor development and drug resistance. MyD88 is abnormally highly expressed in many kinds of malignant tumor cells and tissues.[13,15,16] However, there are other research data showing that MyD88 exerts an antitumor effect. Therefore, there is still no conclusion about the role of MyD88 in the occurrence and development of tumors.[12,13,15,17]

In this study, we studied the expression level of miR-7-5p in ICC tissues and cells and its clinicopathological relationship with ICC cases, and explored the possible mechanism of miR-7-5p inhibiting the migration and invasion of ICC cells.

Table 1. Correlation of mir-7-5p expression with clinicopathological characteristics in intrahepatic cholangiocarcinoma

Variables	Cases, *n*=60	miR-7-5p expression		*p*
		Low, *n*=30	High, *n*=30	
Age in years				0.601
≤55	25	11	14	
>55	35	19	16	
Gender				0.552
Male	45	21	24	
Female	15	9	6	
Tumor stage			0.010*	
T1+T2	40	16	24	
T3+T4	20	14	6	
Lymph node metastasis			0.039*	
Negative	44	18	26	
Positive	16	12	4	
TNM tumor stage			0.013*	
I–II	40	15	25	
III–IV	20	15	5	
MYD 88 expression				0.000*
Low	30	8	22	
High	30	22	8	

*Statistically significant.

Methods

Surgical specimens and clinicopathological data

From January 2013 to January 2018, primary cancer tissues with pathologically confirmed ICC (*n*=60) and their matched adjacent non-tumor tissue samples (ANTs) were obtained at the People's Hospital of Guangxi Zhuang Autonomous Region. The clinical characteristics of the ICC patients are described in Table 1. After surgery, the ICC patients were followed up for 1–70 months. Patients' disease-free survival time was determined from the operation date to the date of recurrent disease diagnosis or the end of follow-up. Overall survival time was determined from the operation date to the date of death or the end of follow-up. All tissues were stored at −80°C prior to use. All tissues were acquired with written informed consent. Our research plans were approved by the Clinical Research Ethics Committee of the People's Hospital of Guangxi Zhuang Autonomous Region (Number: 2013-09), according to the Helsinki Declaration.

Cell culture and transfection

Our study used several ICC cell lines, of which HCCC-9810, HuCCT1, QBC-939, and RBE were purchased from the Shanghai Cell Bank, Chinese Academy of Sciences (Shanghai, China). The human primary intrahepatic biliary epithelial cell line HIBEC was purchased from ATCC (Manassas, VA, USA). All cells were cultured in DMEM (Thermo Fisher, Waltham, MA, USA) according to the manufacturer's recommendations. Hsa-miR-7-5p mimics (miR115129142345-1-5), hsa-miR-7-5p inhibitor (miR2170523092350-1-5) and negative control vector were obtained from RiboBio (Guangzhou, China). MyD88 lentiviral activation particles (sc-417166-ACT) and control lentiviral activation particles (sc-437282) were purchased from Santa Cruz Biotechnology (Dallas, TX, USA). RBE cells were transfected with miR-7-5p mimics or negative control vector, co-transfected with miR-7-5p mimics and MyD88 lentiviral activation particles or control lentiviral activation particles. HIBEC cells were transfected with negative control vector or hsa-miR-7-5p inhibitor. Cells were transfected 24 h before experiments.

Cell counting kit-8 (CCK-8) assay

Two groups of RBE cells were digested with trypsin and seeded into 96-well plates. Approximately 400,000 cells were added to each well. Then, the cells were cultured in the incubator for 24, 48 or 72 h. Next, the cells were exposed to CCK-8 reagent, mixed, and incubated for 1 h. An enzyme-linked immunosorbent detector (Dojindo Molecular Technologies, Kumamoto, Japan) was employed to estimate the absorbance at 450 nm to generate a growth curve.

Flow cytometric analysis of apoptosis

RBE cells were harvested after 48 h, and apoptotic rates were detected by Annexin-V/FITC Kit (BD Biosciences, San Jose, CA, USA). In short, RBE cells were washed with pre-chilled phosphate-buffered saline, added to 1 mL of 1× Annexin V-FITC binding buffer, centrifuged, and (pellet) re-suspended by adding 200 μL binding buffer. RBE cells were then added to 10 μL Annexin V-FITC and 5 μL propidium iodide and incubated for 30 m in the dark. Finally, the apoptotic rate of each group was detected by a FACSCalibur flow cytometer (BD Biosciences). The log of FITC-annexin

V–fluorescence was displayed on the x-axis, and the log of propidium iodide fluorescence was displayed on the y-axis. For each analysis, 10,000 events were recorded.

Transwell chamber assay

Matrigel (BD Biosciences) was added in the upper chamber. RBE cells were trypsinized and resuspended in serum-free medium. Approximately 40,000 cells were added to the upper layer, and 500 μL of Dulbecco's modified Eagle's medium was supplied to the lower layer. After phosphate-buffered saline wash, the noninvasive cells in the upper layer were gently wiped with a wet cotton swab, and the remaining cells were fixed with 4% paraformaldehyde for 20 m. After washing 3 times with phosphate-buffered saline, the cells were stained with 0.1% methyl violet for 25 m. After washing, five fields under the microscope were randomly selected to count the stained cells.

Wound healing assay

The transfected RBE cells or HIBEC cells were seeded into 6-well plates at the density of approximately 500,000. After the cells adhered to 90% confluence, they were uniformly scratched with a 200 μL pipette tip. Then, the cells were observed under a microscope and photographed after the floating cells were removed. After 24 h, they were observed again, and the migration areas were measured in five random fields.

Database analysis

We used the online target gene prediction databases of TargetScan 7.2 (http://www.targetscan.org/vert_72/) and MiRanda (http://www.microrna.org/microrna/home.do) to jointly predict the miR-7-5p target genes, and then the two results were intersected. In addition, target gene databases with experimental verification support, miRTarBase (http://mirtarbase.mbc.nctu.edu.tw) and miRwalk (http://129.206.7.150/), were jointly used to detect possible targets of miR-7-5p. The results were combined as the final miR-7-5p target gene prediction result.

Dual-luciferase reporter gene assay

A luciferase reporter assay with the MyD88 3′-untranslated region (UTR) was used to verify that MyD88 was the direct target of miR-7-5p. The negative control vector or miR-7-5p mimics were co-transfected with the constructed WT-MyD88-3′-UTR (wild-type seed sequence: CUGCCCU) or MT-MyD88-3′-UTR (mutant seed sequence: CUAGGGU) psiCHECK2 reporter vector (Promega, Madison, WI, USA) into RBE cells using Lipofectamine 2000 according to the manufacturer's instructions. Renilla and firefly luciferase activities were assessed with a dual-luciferase reporter gene assay system (Promega).

Western blotting

Total protein were extracted separately from ICC cells. A separation gel and concentrated gel were prepared, and the proteins were separated by electrophoresis and then transferred to membranes. The membranes were blocked with 5% skim milk and incubated with antibodies against MyD88 (1:1,000; Santa Cruz Biotechnology), IRAK4 (1:1,000), TRAF6 (1:1,000), NF-κB (1:1,000), phosphorylated (p)-NF-κB (1:1,000) (all from Cell Signaling Technology, Danvers, MA, USA), GAPDH (1:2,000; Proteintech, Hubei, China) and washed after incubation. Then, the membranes were incubated with goat anti-rabbit/mouse secondary antibody (1:3,000; MultiSciences, Hangzhou, China) at room temperature for 1 h. After being washed, the poly (vinylidene difluoride) membrane was placed in enhanced chemiluminescence reagent and then scanned.

RNA extraction and real-time PCR analysis

Total RNA was extracted from ICC frozen tissues and ICC cell lines by the TRIzol method (Invitrogen, Carlsbad, CA, USA) and stored in a freezer at −80°C. Then, the RNA was reverse transcribed to synthesize complementary DNA by using the miRNA qPCR Detection kit (GeneCopoeia, Rockville, MD, USA) according to the kit instructions. The primer sequences used for quantitative reverse transcription-PCR were as follows: 5′-AAAACTGCTGCCAAAACCAC-3′ (forward) and 5′-GCTGCATTTTACAGCGACCAA-3′ (reverse) for miR-7-5p; 5′-GGCTGCTCTCAACATGCGA-3′ (forward) and 5′-CTGTGTCCGCACGTTCAAGA-3′ (reverse) for MyD88; and 5′-CTCGCTTCGGCAGCACA-3′ (forward) and 5′-AACGCTTCACGAATTTGCGT-3′ (reverse) for U6. MyD88 data were normalized to GAPDH, which was detected using the following primers: 5′-GCACCACCAACTGCTTAGCA-3′ (forward) and 5′-TCTTCTGGGTGGCAGTGATG-3′ (reverse), while U6 was used as an endogenous control for miR-7-5p.

Immunohistochemistry staining of MyD88

The formalin-fixed and paraffin-embedded ICC tissues were cut into 4-μm thick sections, and then we performed antigen retrieval and suppressed endogenous peroxidase activity. MyD88 (1:300; Santa Cruz Biotechnology) was used as the primary antibody to incubate the slides at 4°C overnight, which was followed by incubation with a secondary antibody (1:500; MultiSciences). Finally, the DAB solution was applied to signal generation, and the slides were stained again with hematoxylin and observed by an optical microscope.

Statistical analysis

Data expressed as the mean±standard error of the mean were analyzed by SPSS 22.0 software (IBM Corp., Armonk, NY, USA). Experiments were performed at least three times. We used the chi-square test to explore the correlation between the two variables. For continuous variable analysis, independent *t*-tests and ANOVA test were used. The overall survival and disease-free survival rates of the patients were measured by the Kaplan-Meier method, and the survival rate between the groups were compared by a log-rank test. Prognostic factors were analyzed by univariate analysis and multiple Cox regression modeling. Correlation curves were constructed, and differences between groups were calculated by using Spearman rank correlation analysis. A *p*-value less than 0.05 was considered to indicate a statistically significant difference.

Results

miR-7-5p was down-regulated in ICC tissues and cells

In previous reports, miR-7-5p was often negatively regu-

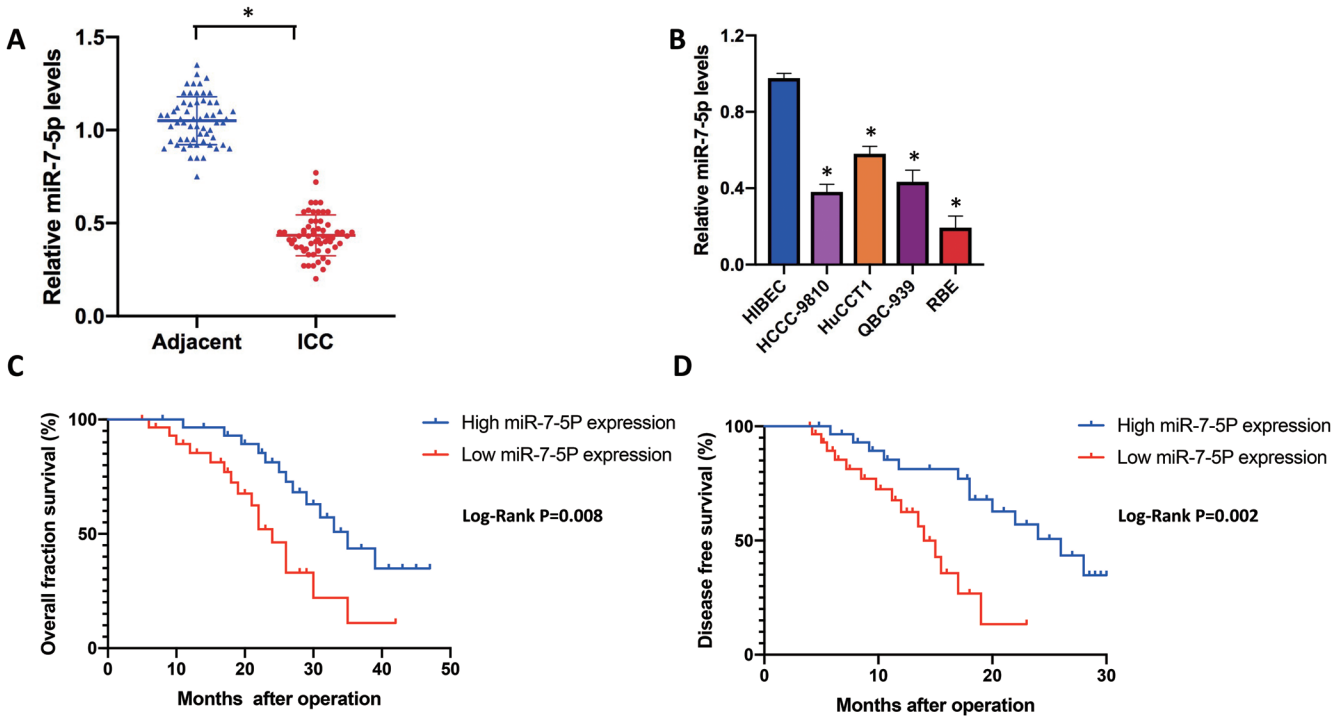

Fig. 1. MiR-7-5p was down-regulated in ICC and related to poor prognosis. (A) Expressions of miR-7-5p were measured by real-time PCR in ICC tissues and their matching matched ANTs. *p<0.001 compared with ANTs. (B) The expression of miR-7-5p in ICC cell lines (QBC-939, HuCCT1, RBE, HCCC-9810) and a normal cell line (HIBEC). *p<0.001 compared with the HIBEC cell line. (C, D) The overall survival rate and disease-free survival rate were calculated by the Kaplan-Meier method. Data are presented as the mean±standard deviation. ANTs, adjacent non-tumor tissue samples; ICC, intrahepatic cholangiocarcinoma.

lated in ICC tissues. To further verify this observation, we first measured the expression of miR-7-5p (written as miR-7 hereafter for conciseness) in 60 pairs of ICC tissues and ANTs by real-time PCR. Notable down-regulation of miR-7 was observed in ICC tissues compared with the matched ANTs (Fig. 1A). To explore whether miR-7 was dysregulated in ICC cells, the expression of miR-7 in ICC cell lines (HCCC-9810, HuCCT1, QBC-939, RBE) and normal HIBEC cells were quantified. We confirmed that the expression of miR-7 was also reduced in ICC cell lines compared with HIBEC cells (Fig. 1B). Therefore, we demonstrated the frequent down-regulation of miR-7 in ICC.

Down-regulation of miR-7 was related to poor prognosis

To reveal the clinico-pathological characteristics of miR-7 in ICC, we divided ICC patients into two groups according to the median expression of miR-7: the miR-7 low expression group (n=30) and the miR-7 high expression group (n=30). The results showed that the low expression of miR-7 was related to higher tumor grade, more positive lymph node metastasis, and higher clinical stage (Table 1). Because poorer cellular differentiation and advanced tumor stage were related to ICC metastasis, the down-regulation of miR-7 may participate in the metastatic growth of ICC. In addition, we also investigated the relationship between low miR-7 expression and patients' survival. After 3 years of follow-up, we found that the 1-year disease-free survival rates and 3-year overall survival rates of patients in the low miR-7 expression group were notably poorer than those in the high expression group (Fig. 1C, D). All the above data revealed that the loss of miR-7 expression may play a role in the progression of ICC and causing the poor prognosis of ICC patients.

miR-7 negatively regulated RBE cell proliferation, migration, and invasion and induced apoptosis

We observed that the deletion of miR-7 was closely correlated with the metastasis and prognosis of ICC; further, we analyzed the effect of miR-7 on ICC cell proliferation, migration and invasion. Because miR-7 had the lowest expression in RBE cells, we first constructed a stable expression of miR-7. Compared with the negative control group, miR-7 expression was confirmed to notably increase in the miR-7 mimic transfection group (Fig. 2A). Through the CCK-8 assay, we observed that miR-7 re-expression notably inhibited RBE cell proliferation *in vitro* (Fig. 2B). We then used flow cytometry to reveal the effect of miR-7 re-expression on apoptotic rates. The data indicated that the apoptotic rate of RBE cells also increased markedly with increasing miR-7 expression, which demonstrated that miR-7 induced cell apoptosis in ICC (Fig. 2C). In the Transwell cell invasion assay, overexpression of miR-7 reduced the cells which invaded the lower chamber (Fig. 2D). Similarly, in the miR-7 high expression group, the ability of cells to migrate was notably impeded compared with that in the low expression group (Fig. 2E). To further detect the effects of miR-7 on cell migration and invasive ability, HIBEC cells expressing relatively high endogenous miR-7 were transfected with miR-7 inhibitors. The down-regulation of miR-7 was verified by quantitative reverse transcription-PCR (Fig. 2F). Interestingly, inhibition of miR-7 markedly promoted cell invasion (Fig. 2G) and migration in HIBEC cells (Fig. 2H). Our prior studies demonstrated that miR-7 suppressed ICC metasta-

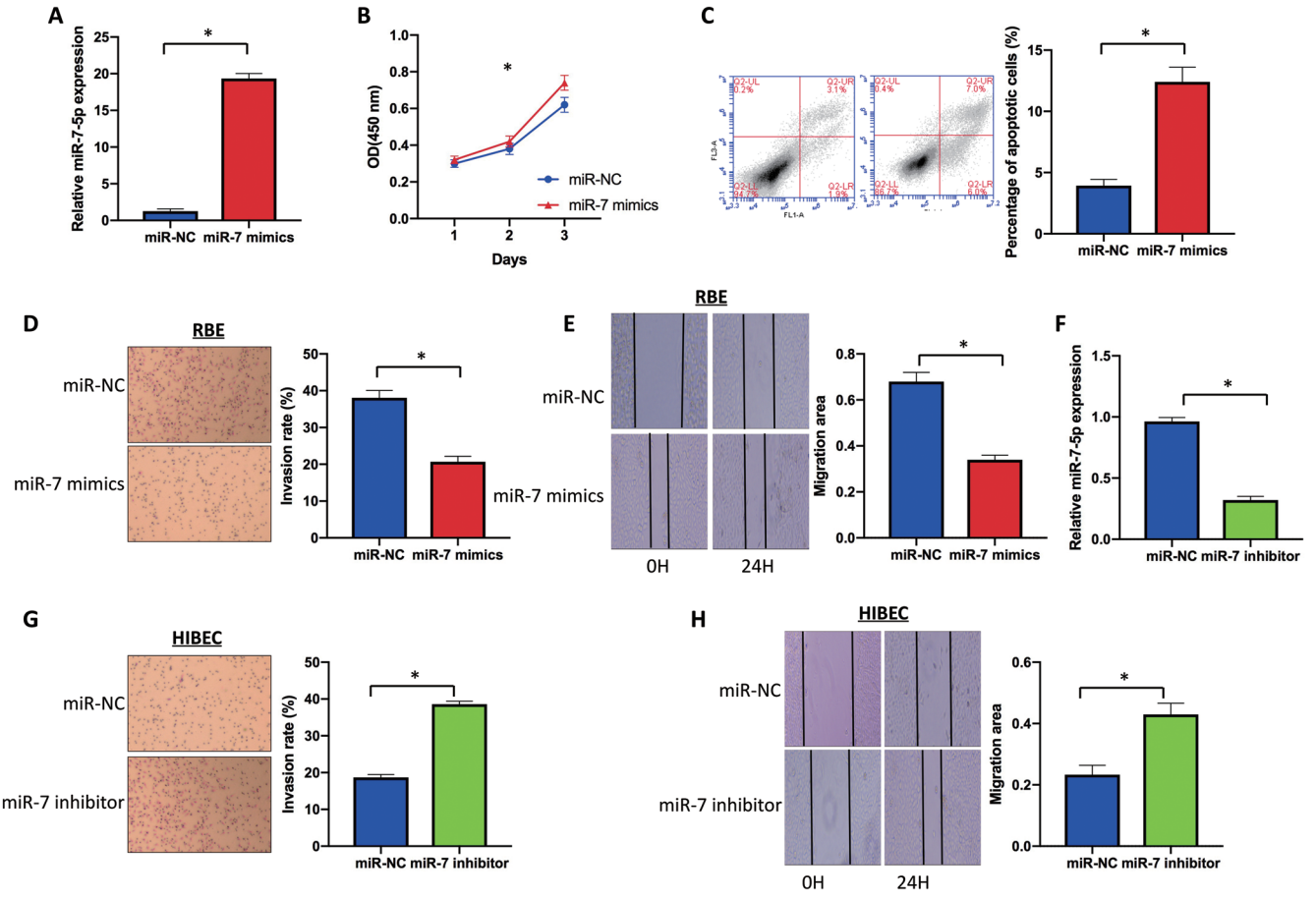

Fig. 2. MiR-7 inhibited proliferation, migration, and invasion and induced apoptosis in ICC cell line. (A) MiR-7-5p mimics and negative control were efficiently transfected into RBE cells. (B) Cell proliferation rates were measured in RBE cells of two groups through CCK-8 assay after 24, 48 and 72 h. (C) Flow cytometric analysis was used to identify apoptotic rates of RBE cells. (D) Invasive abilities of RBE cells after transfection were identified by the Transwell assay (magnification, ×200). (E) Migration rates of RBE cells were determined by wound healing assay. (F) The expression of miR-7-5p was measured in HIBEC cells transfected with miR-7-5p inhibitor and negative control. (G) Invasive abilities of HIBEC cells after transfection were confirmed by the Transwell assay (magnification, ×200). (H) Migration rates of HIBEC cells were confirmed by wound healing assay. *p<0.05 and ***p<0.001 compared with the NC group. Data are presented as the mean±standard deviation. CCK-8, cell counting kit-8; ICC, intrahepatic cholangiocarcinoma.

sis by negatively regulating cell proliferation, migration, and invasion and inducing cell apoptosis.

MyD88 was a direct target of miR-7 in RBE cells

Previous research results revealed that miR-7 functions as a tumor suppressor gene in ICC. Accordingly, we further sought to identify the underlying targets of miR-7 that were related to tumor metastasis. We explored miR-7 downstream gene targets through four different miRNA targeting prediction tools: TargetScan, MiRanda, miRTarBase and miRwalk. A potential candidate target gene, MyD88, was then selected, which had a predicted consequential pairing with miR-7 at bases 55–61 (Fig. 3A). To further explore whether the anti-metastatic properties of miR-7 in ICC were related to MyD88, we first performed a dual-luciferase reporter gene assay in RBE cells. The luciferase activity of RBE cells with wild-type MyD88 after transfection with miR-7 mimics was markedly reduced compared with that of the mimic NC-transfected cells. However, in RBE cells with mutated MyD88, the decrease in luciferase activity was significantly reversed (Fig. 3B). We further verified whether miR-7 could regulate MyD88 expression at the cellular level. After transfection with miR-7 mimics, the MyD88 level of RBE cells was decreased by approximately 50% (Fig. 3C). The inhibition of miR-7 in normal HIBEC cells markedly increased MyD88 expression (Fig. 3D). Accordingly, MyD88 was proven to be a novel target of miR-7 in RBE cells.

Overexpression of MyD88 counteracted the effects of miR-7 in RBE cells

Previous findings indicated that miR-7 inhibits metastasis by negatively regulating ICC cell migration and invasion and that MyD88 was directly targeted by miR-7. Therefore, we suspected that MyD88 may participate in miR-7-mediated anti-metastatic properties. To verify that miR-7 directly targets MyD88 to perform its function, miR-7-transfected RBE cells were infected with MyD88 lentiviral activation particles or control lentiviral activation particles. MyD88 protein levels were significantly increased by transfection of MyD88 lentiviral activation particles (Fig. 4A), and mRNA levels exhibited the same trend with quantitative reverse transcription-PCR detection (Fig. 4B). In wound healing assays, the recovery of MyD88 expression partially promoted the migration of RBE cells overexpressing miR-7 (Fig.

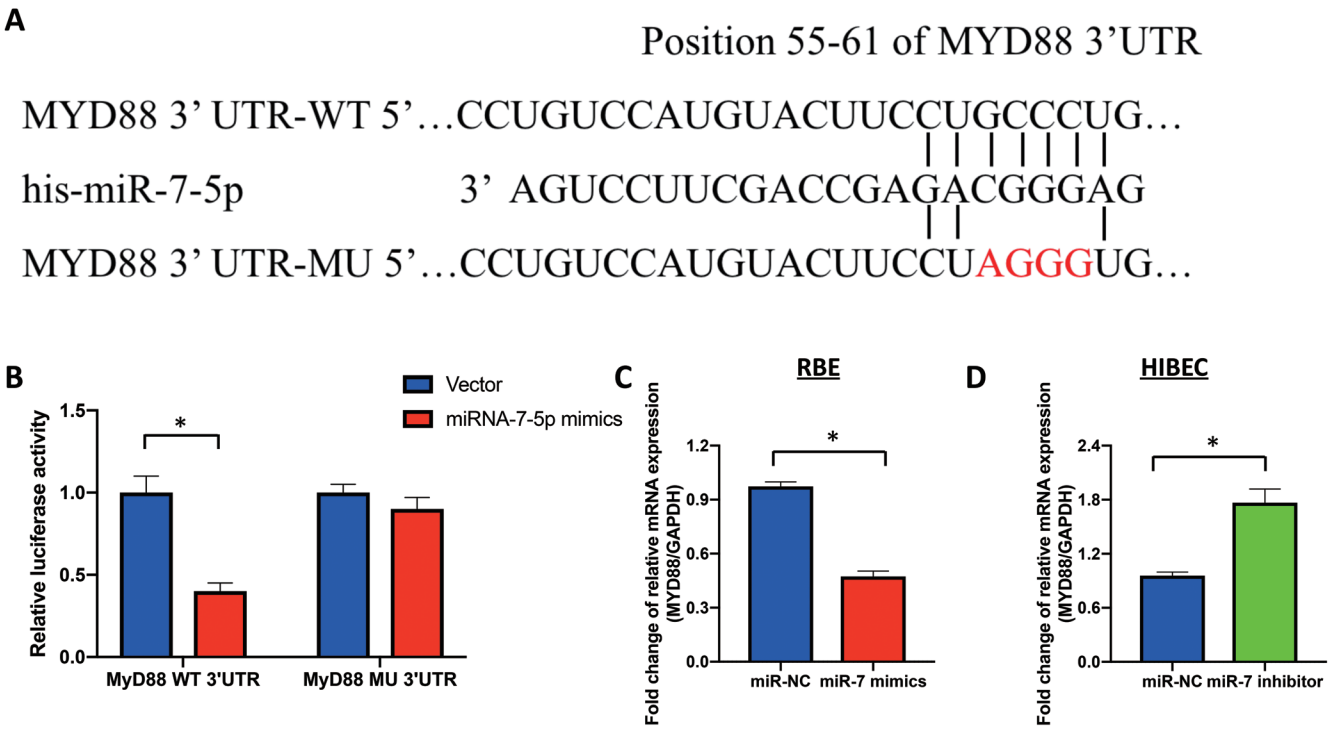

Fig. 3. MyD88 was proven to be a novel target of miR-7-5p in RBE cells. (A) MyD88 has a predicted consequential pairing with miR-7-5p at bases 55–61. psiCHECK2 dual-luciferase reporter vectors containing wild-type (WT) or mutant (MT) MyD88 3′-UTR were constructed. (B) Renilla luciferase activity was standardized to firefly luciferase activity in RBE cells with WT-MyD88 or MT-MyD88. (C) After transfection with miR-7 mimics, the MyD88 level of RBE cells was decreased significantly. (D) QRT-PCR was performed to identify the expression level of MyD88 in HIBEC cells. *p<0.05 and ***p<0.001 compared with the NC group. Data are presented as the mean±standard deviation.

4C). In Transwell assays, increased expression of MyD88 enhanced the invasion ability of miR-7-overexpressing RBE cells, which was suppressed by miR-7 (Fig. 4D). Accordingly, the findings showed that miR-7 inhibited migration and invasion by targeting MyD88, and the underlying mechanism was further studied. The IRAK4/TRAF6/NF-κB signaling pathways, which had been reported to be important pathways for regulating the differentiation, survival, and movement of normal and cancer cells, were closely related to the physiological role of MyD88. Therefore, we further investigated the influences of miR-7 and MyD88 on the expression changes of IRAK4, TRAF6, NF-κB and p-NF-κB. Western blotting analysis revealed that overexpression of miR-7 suppressed IRAK4 and TRAF6 protein expression and negatively regulated NF-κB phosphorylation. The restoration of MyD88 expression in RBE cells notably reversed the inhibitory effects of miR-7 (Fig. 4E). All these results suggested that miR-7 inhibited invasion and metastasis by directly targeting MyD88, possibly through IRAK4/TRAF6/NF-κB/MyD88 signaling pathways.

MyD88 was significantly overexpressed in ICC and negatively correlated with the expression of miR-7

Due to the promoting effect of MyD88 in many tumors, we first determined the expression of MyD88 in ICC tissues. ICC tissues showed significantly higher expression of MyD88 than ANTs (Fig. 5A). Interestingly, we also found a negative correlation between miR-7 and MyD88 expression (Fig. 5B). Furthermore, we examined the expression of MyD88 in ICC cell lines. The expression level of MyD88 was confirmed to be increased in all ICC cell lines through quantitative reverse transcription-PCR, with the highest expression in RBE and QBC-939 cells (Fig. 5C). We further quantified the expression levels of MyD88 in ICC tissues with different miR-7 levels by immunohistochemistry (Fig. 5D). Tumors with lower levels of miR-7 tended to overexpress MyD88, and conversely, tumors that overexpressed miR-7 showed a lower level of MyD88. After 3 years of follow-up, we found that the 1-year disease-free survival rates and 3-year overall survival rates of patients in the high MyD88 expression group were notably poorer than those in the low expression group (Fig. 5E, F). Univariate Cox proportional hazard regression analyses showed that tumor-necrosis-metastasis (known as TNM) stage, miR-7-5p expression, and MyD88 expression were prognostic factors of ICC (p<0.05). See Table 2 for details. Including TNM tumor stage, miR-7-5p expression, and MyD88 expression into the Cox model and performing multivariate analysis showed that MyD88 expression (odds ratio: 3.834, 95% confidence interval: 1.435–10.239, p<0.05) was an independent factor affecting prognosis. Collectively, these data suggested that dysregulation of miR-7 was related to the overexpression of MyD88 in ICC and high MyD88 expression was related to poor prognosis of ICC.

Discussion

ICC is a malignant tumor derived from the bile duct epithelium and ranks second among the primary liver cancers.[1,18] The difference between ICC and extrahepatic cholangiocarcinoma is that ICC occurs in the liver parenchyma. Although the incidence of ICC worldwide is much lower than that of hepatocellular carcinoma (HCC), some recent studies have

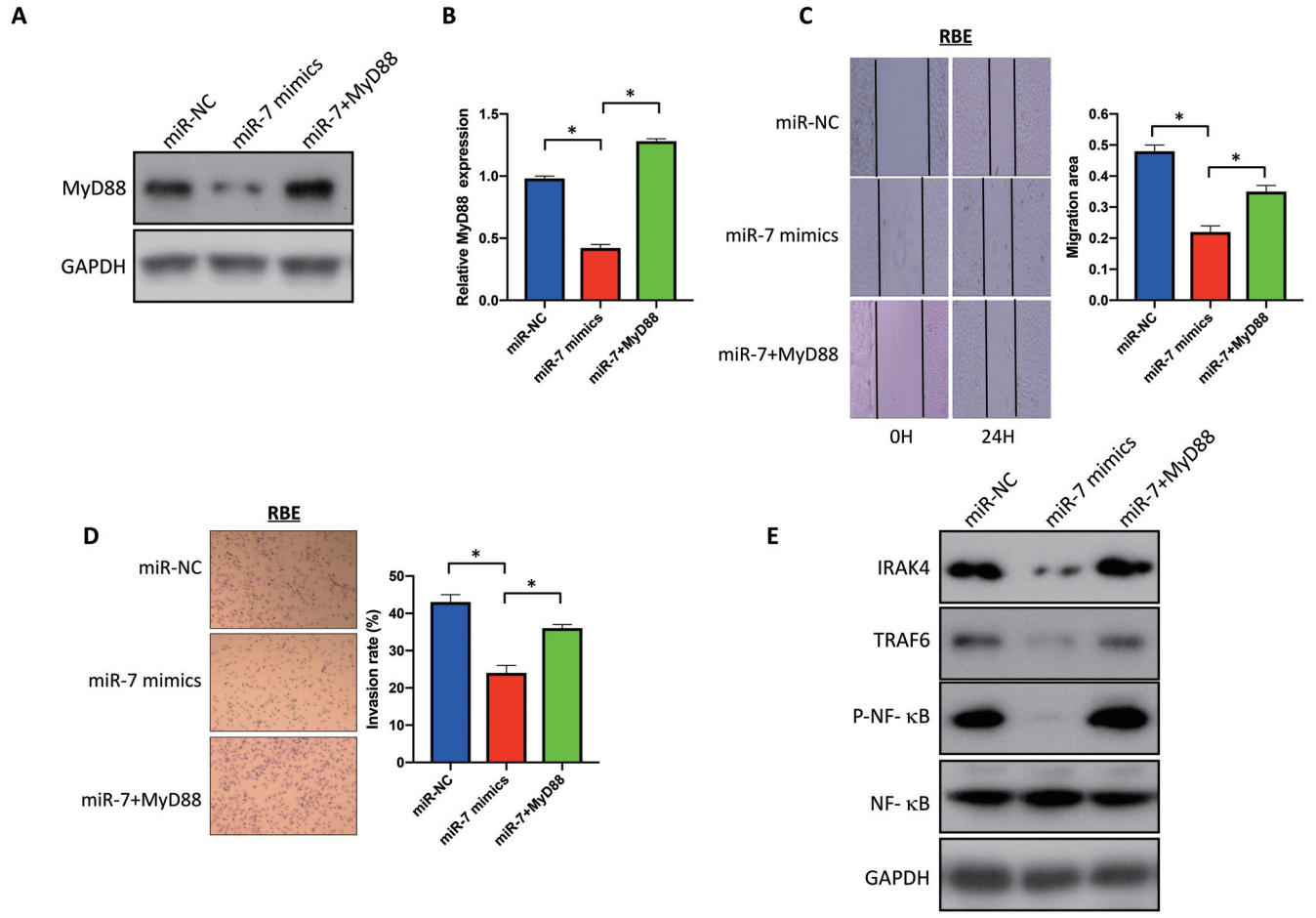

Fig. 4. Overexpression of MyD88 counteracted the effects of miR-7-5p in RBE cells. (A) MyD88 protein levels of different groups were evaluated, as detected by western blotting in RBE cells. (B) MyD88 levels were measured by qRT-PCR in RBE cells. (C) Migration rates of RBE cells were confirmed by wound healing assay. (D) Invasive abilities of RBE cells after transfection were measured by Transwell assay (magnification, ×200). (E) Western blotting analysis of the protein expression of IRAK4, TRAF6, NF-κB and p-NF-κB. *p<0.05 and ***p<0.001 compared with the NC group. Data are presented as the mean±standard deviation.

shown that the incidence of ICC has increased rapidly in the past few decades, and the mortality rate is still high.[19] The only potentially curative treatment for ICC is radical surgery.[6,7,20] However, less than 30% of patients undergo surgical resection because the early diagnosis rate of ICC is very low. Moreover, the 5-year survival rate after ICC surgical resection is less than 45%, and the recurrence rate is about 50% from most clinical studies. Most patients have lost the opportunity for radical surgery.[21,22] For patients with advanced unresectable and metastatic ICC, the standard first-line systemic treatment is gemcitabine combined with cisplatin. But the therapeutic effect is very limited, and the overall survival time is less than 1 year.[22] New effective treatment methods are urgently required for ICC patients.

MiR-7 plays a role in the diagnosis, prognosis, anti-metastasis and treatment of various cancers via targeting different genes in various complex ways. MiR-7 can induce rhabdomyosarcoma cell necrosis and apoptosis via mitochondrial damage.[23] MiR-7-5p also can modulate malignant phenotypes of T cell acute lymphoblastic leukemia (referred to as T-ALL) cells and serve as a potential therapeutic target for T-ALL.[24] Moreover, miR-7 acts as a tumor suppressor in digestive system malignancies.[25] MiR-7 is down-regulated in HCC, which directly targets the tumor suppressor gene CUL5 towards involvement in the progression of HCC.[26] MiR-7 is also down-regulated in colorectal cancer to negatively regulate the tumorigenesis gene PAX6 towards involvement in the progression of colorectal cancer.[27] These studies show that miR-7 can play an anti-tumor role in digestive system tumors by acting on various key genes.

ICC are clinically characterized by poor prognosis, partly due to tumor angiogenesis via VEGF overexpression.[28] In liver cancer, it has been found that over-activated TLR4/MyD88 can up-regulate the expression of VEGF and participate in tumor progression in HCC.[29] But the role of MyD88 in ICC is temporarily poorly understood. Meanwhile, it is reported that the MyD88 signaling could play dual functional roles in colorectal cancer. Sometimes, it plays the tumor-promoting role that enhances cancer inflammation and intestinal flora imbalance to induce tumor invasion and tumor cell self-renewal; at other times, it plays an anti-tumor role that helps to maintain the host-microbiota homeostasis to induce tumor cell cycle arrest and immune responses against cancer cells.[13] Thus, studying the role of MyD88 in cholangiocarcinoma is not only interesting but also meaningful. More and more reports indicate that MyD88 combined with NF-κB promotes tumor development. NF-κB is one of the important signaling molecules downstream of MyD88.[30,31] Notably, we confirmed that MyD88 was not only increased in many ICC cell lines but also significantly higher in ICC tissues than in ANTs. MyD88 was then predicted to be a downstream gene target of miR-7 by four different

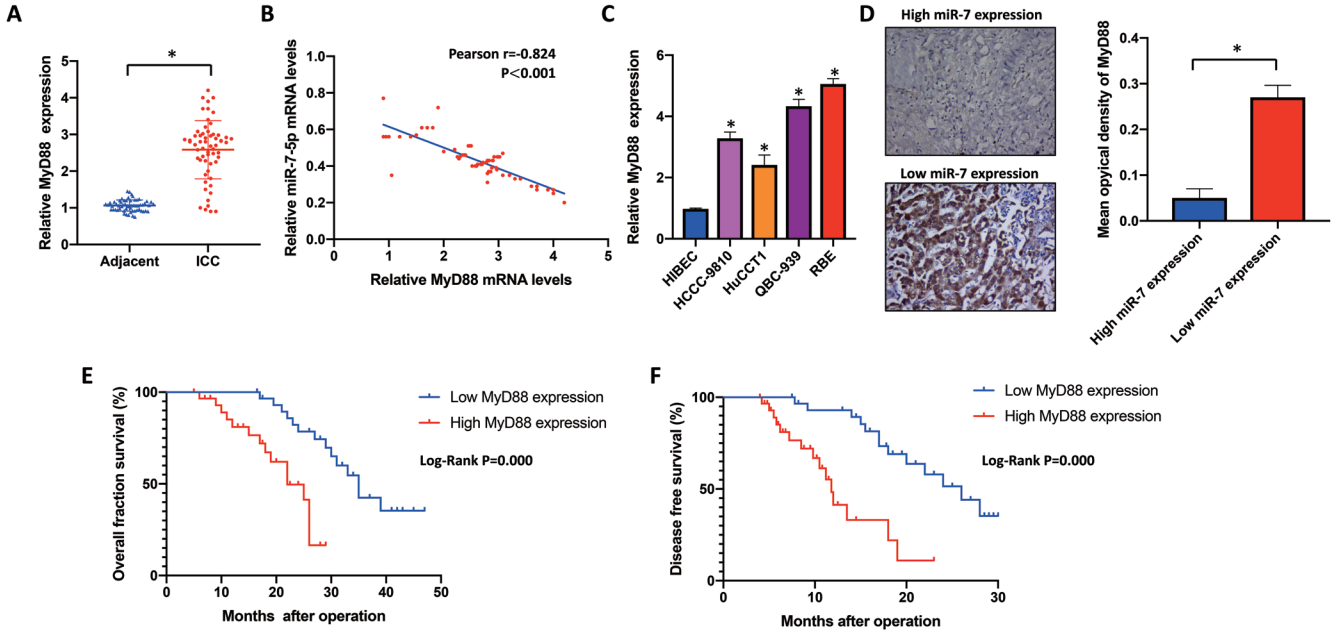

Fig. 5. MyD88 was significantly upregulated in ICC tissues and negatively correlated with miR-7 in ICC. (A) Real-time PCR was performed to identify the mRNA levels of MyD88 in ICC tissues and their matching ANTs (n=75). ***p<0.001 compared with ANTs. (B) In ICC tissues, the levels of MyD88 were negatively correlated with miR-7-5p (n=75). (C) MyD88 mRNA levels of ICC cell lines and HIBEC cells were identified. *p<0.05 compared with HIBEC cells. (D) Representative pictures of MyD88 immunohistochemistry in ICC tissues with different miR-7 levels. (E, F) The 1-year disease-free survival rates and 3-year overall survival rates of patients in the high MyD88 expression group were notably poorer than those in the low expression group. Data are presented as the mean±standard deviation. ANTs, adjacent non-tumor tissue samples; ICC, intrahepatic cholangiocarcinoma.

miRNA targeting prediction tools, and the targeting relationship was confirmed through a dual-luciferase reporter gene assay. Interestingly, the present data revealed that miR-7 was negatively correlated with MyD88 in ICC tissues. Tumors with lower levels of miR-7 tended to overexpress MyD88, and conversely, tumors that overexpressed miR-7 showed a lower level of MyD88. MyD88 expression was an independent factor affecting prognosis. Furthermore, restoration of MyD88 rescued miR-7-inhibited tumor migration and invasion. All the findings showed that miR-7 inhibits tumor metastasis by targeting MyD88 *in vitro*.

Previous studies have shown that MyD88 is required for IRAK4/TRAF6/NF-κB signaling, which plays a pivotal role in the phenotypic changes, invasion and metastasis of malignant tumor cells by promoting epithelial-mesenchymal transition (commonly referred to as EMT) and local adhesion dynamics.[16–18] Overexpression of MyD88 is involved in activating NF-κB, inducing cell proliferation, anti-apoptosis, and promoting cell EMT. With increased p-NF-κB expression levels, cell migration and invasion capabilities are enhanced.[32] Therefore, we further detected the influences of miR-7 and MyD88 on the expression changes of IRAK4, TRAF6, NF-κB and p-NF-κB. We confirmed that up-regulation of miR-7 inhibited IRAK4 and TRAF6 protein expression and negatively regulated the phosphorylation of NF-κB. The restoration of MyD88 in RBE cells notably reversed inhibitory effects of miR-7. Therefore, we postulated that miR-7 could inhibit invasion and metastasis in ICC by directly targeting MyD88, possibly through IRAK4/TRAF6/MyD88 signaling pathways. Further research investigations are needed to adequately illuminate the miR-7/MyD88-related signaling pathway and its functions in ICC.

miR-7 was confirmed to significantly inhibit metastasis by down-regulating MyD88 *in vitro.* Similarly, Shen *et al*.[33] demonstrated that miR-7 inhibited invasion in colorectal cancer by regulating the twist family bHLH transcription

Table 2. Multivariate analysis of factors contributing to overall survival in intrahepatic cholangiocarcinoma patients

Variables	Univariate analysis		Multivariate analysis	
	HR (95% CI)	*p*	HR (95% CI)	*p*
Age, ≤55 vs. >55	0.308 (0.034–2.806)	0.296	–	–
Gender, female vs. male	2.863 (0.870–9.420)	0.083	–	–
Tumor stage, T1+T2 vs. T3+T4	0.473 (0.102–2.189)	0.338	–	–
Lymph node metastasis, negative vs. positive	0.308 (0.034–2.806)	0.296	–	–
TNM tumor stage, I–II vs. III–IV	3.366 (0.841–13.473)	0.046	3.863 (1.870–9.420)	0.483
miR-7-5p expression, low vs. high	0.276(0.087–0.869)	0.028	0.609 (0.261–1.421)	0.235
MYD 88 expression, low vs. high	3.767 (1.240–11.447)	0.019	3.834 (1.435–10.239)	0.007

Univariate and multivariate analysis of prognostic factors in ICC patients included in the survival analysis. Statistical analyses were performed by Cox proportional hazards regression. A *p*-value <0.05 was considered significant. Italic indicates significant *p* values. CI, confidence interval; HR, hazard ratio.

factor 1 and the down-regulation of miR-7, promoting lung metastasis. The prior studies showed that miR-7 could act as a tumor suppressor in many types of malignancies.

In summary, we confirmed the down-regulation of miR-7-5p in ICC, which was related to poor prognosis. miR-7-5p inhibited invasion and metastasis *in vitro* by directly targeting MyD88, indicating that miR-7-5p and MyD88 could be novel targets for preventing ICC metastasis in the future.

Funding

None to declare.

Conflict of interest

The authors have no conflict of interests related to this publication.

Author contributions

Conception and design of the project (YtT, ZT), performance of experiments, obtainment and analysis of data (YT, JY), writing of the manuscript (TL), critical revision of the manuscript (YtT, ZT). All authors read and approved the final manuscript.

Ethics approval and consent to participate

All tissues used in this study were acquired with written informed consent. All human experiments were approved by the Clinical Research Ethics Committee of the People's Hospital of Guangxi Zhuang Autonomous Region (No. 2013-09). All protocols involving the use of animals were approved by the Animal Experimental Ethical Inspection of the People's Hospital of Guangxi Zhuang Autonomous Region.

Data sharing statement

The datasets used and analyzed during the current study are available from the corresponding author, upon reasonable request.

References

[1] Yu TH, Chen X, Zhang XH, Zhang EC, Sun CX. Clinicopathological characteristics and prognostic factors for intrahepatic cholangiocarcinoma: a population-based study. Sci Rep 2021;11(1):3990. doi:10.1038/s41598-021-83149-5.
[2] Peery AF, Crockett SD, Murphy CC, Lund JL, Dellon ES, Williams JL, *et al*. Burden and cost of gastrointestinal, liver, and pancreatic diseases in the United States: update 2018. Gastroenterology 2019;156(1):254–272.e11. doi:10.1053/j.gastro.2018.08.063.
[3] Brandi G, Venturi M, Pantaleo MA, Ercolani G; GICO. Cholangiocarcinoma: current opinion on clinical practice diagnostic and therapeutic algorithms: a review of the literature and a long-standing experience of a referral center. Dig Liver Dis 2016;48(3):231–241. doi:10.1016/j.dld.2015.11.017.
[4] Wei F. Preoperative model and patient selection for neoadjuvant therapy for intrahepatic cholangiocarcinoma. JAMA Surg 2021;156(4):395. doi:10.1001/jamasurg.2020.6182.
[5] Liu S, Jiang B, Li H, He Z, Lv P, Peng C, *et al*. Wip1 is associated with tumorigenity and metastasis through MMP-2 in human intrahepatic cholangiocarcinoma. Oncotarget 2017;8(34):56672–56683. doi:10.18632/oncotarget.18074.
[6] Liu S, Jiang J, Huang L, Jiang Y, Yu N, Liu X, *et al*. iNOS is associated with tumorigenicity as an independent prognosticator in human intrahepatic cholangiocarcinoma. Cancer Manag Res 2019;11:8005–8022. doi:10.2147/CMAR.S208773.
[7] Chen C, Jiang J, Fang M, Zhou L, Chen Y, Zhou J, *et al*. MicroRNA-129-2-3p directly targets Wip1 to suppress the proliferation and invasion of intrahepatic cholangiocarcinoma. J Cancer 2020;11(11):3216–3224. doi:10.7150/jca.41492.
[8] Yang X, Xie X, Xiao YF, Xie R, Hu CJ, Tang B, *et al*. The emergence of long non-coding RNAs in the tumorigenesis of hepatocellular carcinoma. Cancer Lett 2015;360(2):119–124. doi:10.1016/j.canlet.2015.02.035.
[9] Shi Y, Luo X, Li P, Tan J, Wang X, Xiang T, *et al*. miR-7-5p suppresses cell proliferation and induces apoptosis of breast cancer cells mainly by targeting REGgamma. Cancer Lett 2015;358(1):27–36. doi:10.1016/j.canlet.2014.12.014.
[10] Zhu W, Wang Y, Zhang D, Yu X, Leng X. MiR-7-5p functions as a tumor suppressor by targeting SOX18 in pancreatic ductal adenocarcinoma. Biochem Biophys Res Commun 2018;497(4):963–970. doi:10.1016/j.bbrc.2018.02.005.
[11] Li G, Huang M, Cai Y, Yang Y, Sun X, Ke Y. Circ-U2AF1 promotes human glioma via derepressing neuro-oncological ventral antigen 2 by sponging hsa-miR-7-5p. J Cell Physiol 2019;234(6):9144–9155. doi:10.1002/jcp.27591.
[12] Maeda Y, Echizen K, Oshima H, Yu L, Sakulsak N, Hirose O, *et al*. Myeloid differentiation factor 88 signaling in bone marrow-derived cells promotes gastric tumorigenesis by generation of inflammatory microenvironment. Cancer Prev Res (Phila) 2016;9(3):253–263. doi:10.1158/1940-6207.CAPR-15-0315.
[13] Wang L, Yu K, Zhang X, Yu S. Dual functional roles of the MyD88 signaling in colorectal cancer development. Biomed Pharmacother 2018;107:177–184. doi:10.1016/j.biopha.2018.07.139.
[14] Bajo M, Patel RR, Hedges DM, Varodayan FP, Vlkolinsky R, Davis TD, *et al*. Role of MyD88 in IL-1beta and ethanol modulation of GABAergic transmission in the central amygdala. Brain Sci 2019;9(12):361. doi:10.3390/brainsci9120361.
[15] Liang B, Chen R, Wang T, Cao L, Liu Y, Yin F, *et al*. Myeloid differentiation factor 88 promotes growth and metastasis of human hepatocellular carcinoma. Clin Cancer Res 2013;19(11):2905–2916. doi:10.1158/1078-0432.CCR-12-1245.
[16] Kennedy CL, Najdovska M, Tye H, McLeod L, Yu L, Jarnicki A, *et al*. Differential role of MyD88 and Mal/TIRAP in TLR2-mediated gastric tumourigenesis. Oncogene 2014;33(19):2540–2546. doi:10.1038/onc.2013.205.
[17] Pradere JP, Dapito DH, Schwabe RF. The Yin and Yang of Toll-like receptors in cancer. Oncogene 2014;33(27):3485–3495. doi:10.1038/onc.2013.302.
[18] Rizvi S, Khan SA, Hallemeier CL, Kelley RK, Gores GJ. Cholangiocarcinoma - evolving concepts and therapeutic strategies. Nat Rev Clin Oncol 2018;15(2):95–111. doi:10.1038/nrclinonc.2017.157.
[19] Seehawer M, D'Artista L, Zender L. The worst from both worlds: cHCC-ICC. Cancer Cell 2019;35(6):823–824. doi:10.1016/j.ccell.2019.05.008.
[20] Liu S, Liu X, Li X, Li O, Yi W, Khan J, *et al*. Application of laparoscopic radical resection for type III and IV hilar cholangiocarcinoma treatment. Gastroenterol Res Pract 2020;2020:1506275. doi:10.1155/2020/1506275.
[21] Goeppert B, Toth R, Singer S, Albrecht T, Lipka DB, Lutsik P, *et al*. Integrative analysis defines distinct prognostic subgroups of intrahepatic cholangiocarcinoma. Hepatology 2019;69(5):2091–2106. doi:10.1002/hep.30493.
[22] Gourd E. Derazantinib for intrahepatic cholangiocarcinoma. Lancet Oncol 2019;20(1):e11. doi:10.1016/S1470-2045(18)30891-X.
[23] Yang L, Kong D, He M, Gong J, Nie Y, Tai S, *et al*. MiR-7 mediates mitochondrial impairment to trigger apoptosis and necroptosis in rhabdomyosarcoma. Biochim Biophys Acta Mol Cell Res 2020;1867(12):118826. doi:10.1016/j.bbamcr.2020.118826.
[24] Li G, Gao L, Zhao J, Liu D, Li H, Hu M. LncRNA ANRIL/miR-7-5p/TCF4 axis contributes to the progression of T cell acute lymphoblastic leukemia. Cancer Cell Int 2020;20:335. doi:10.1186/s12935-020-01376-8.
[25] Chen WQ, Hu L, Chen GX, Deng HX. Role of microRNA-7 in digestive system malignancy. World J Gastrointest Oncol 2016;8(1):121–127. doi:10.4251/wjgo.v8.i1.121.
[26] Ma C, Qi Y, Shao L, Liu M, Li X, Tang H. Downregulation of miR-7 upregulates Cullin 5 (CUL5) to facilitate G1/S transition in human hepatocellular carcinoma cells. IUBMB Life 2013;65(12):1026–1034. doi:10.1002/iub.1231.
[27] Li Y, Li Y, Liu Y, Xie P, Li F, Li G. PAX6, a novel target of microRNA-7, promotes cellular proliferation and invasion in human colorectal cancer cells. Dig Dis Sci 2014;59(3):598–606. doi:10.1007/s10620-013-2929-x.
[28] Simone V, Brunetti O, Lupo L, Testini M, Maiorano E, Simone M, *et al*. Targeting angiogenesis in biliary tract cancers: an open option. Int J Mol Sci 2017;18(2):418. doi:10.3390/ijms18020418.
[29] Zhang C, Wang N, Tan HY, Guo W, Chen F, Zhong Z, *et al*. Direct inhibition of the TLR4/MyD88 pathway by geniposide suppresses HIF-1α-independent VEGF expression and angiogenesis in hepatocellular carcinoma. Br J Pharmacol 2020;177(14):3240–3257. doi:10.1111/bph.15046.
[30] Zhu G, Cheng Z, Huang Y, Zheng W, Yang S, Lin C, *et al*. MyD88 mediates colorectal cancer cell proliferation, migration and invasion via NF-κB/AP-1 signaling pathway. Int J Mol Med 2020;45(1):131–140. doi:10.3892/ijmm.2019.4390.
[31] Jin X, Shi Q, Li Q, Zhou L, Wang J, Jiang L, *et al*. CRL3-SPOP ubiquitin ligase complex suppresses the growth of diffuse large B-cell lymphoma by negatively regulating the MyD88/NF-κB signaling. Leukemia 2020;34(5):1305–1314. doi:10.1038/s41375-019-0661-z.
[32] Salcedo R, Cataisson C, Hasan U, Yuspa SH, Trinchieri G. MyD88 and its divergent toll in carcinogenesis. Trends Immunol 2013;34(8):379–389. doi:10.1016/j.it.2013.03.008.
[33] de Almeida BC, Garcia N, Maffazioli G, dos Anjos LG, Baracat EC, Carvalho KC. Oncomirs expression profiling in uterine leiomyosarcoma cells. Int J Mol Sci 2017;19(1):52. doi:10.3390/ijms19010052.